Available online at www.sciencedirect.com

ScienceDirect

Transportation Research Procedia 70 (2023) 356–363

Transportation Research Procedia

www.elsevier.com/locate/procedia

8th International Electric Vehicle Conference (EVC 2023)

Load Monitoring Based on Monte Carlo Simulation for the Identification of Fast Charging Stations

Sami M. Alshareef[a]*

[a]*Department of Electrical Engineering, College of Engineering, Jouf University, Saudi Arabia*

Abstract

In this paper, four EV fast chargers are assumed to be located at the parking lot of a commercial facility, namely a supermarket. The supermarket consists of different centers that provide different services at different hours of operation. The Monte Carlo Simulation method is utilized to estimate the power profile of the commercial load. Both the commercial load and the fast charging station (FCS) are connected to the main grid at the point of common coupling (PCC). The aim of this paper is to apply load disaggregation using a single point sensing at the PCC to manage the system's energy by proposing a machine learning-based method for detecting and classifying the four EV fast chargers rated 50 kW, 90 kW, 150 kW, and 350 kW, respectively. The commercial load can be considered as a background load disturbing the disaggregation process at the PCC. The voltage and current signals are monitored at the PCC and utilized by Fourier transform to determine three features: the change of the active, reactive, and apparent power. Two machine learning classifiers, i.e., Kernel Naive Bayes (KNB) and k-Nearest Neighbors (KNN), are introduced in order to develop the appropriate prediction models. The results reveal that the KNB outperforms the KNN based on the mean classification accuracy as well as the F-measure index.

Keywords: Load disaggregation, fast charging station, energy management, electric vehcile, commercial load ;

1. Introduction

The interconnection of high penetration levels of electric vehicles (EVs) and their infrastructures could overload power grid components, such as transformers and cables. Furthermore, the fast-charging mechanism of EVs exacerbates the situation as such charging drains high levels of power from the power network, thus stressing the local grid. The aim of this current work is to manage the system's energy by detecting individual fast charger operations

* Corresponding author. Tel.: +966146544956; fax: +966146544901.
E-mail address: smalshareef@ju.edu.sa

2352-1465
10.1016/j.trpro.2023.11.040

using single point sensing for non-intrusive load monitoring and load disaggregation at EV fast charging points in the commercial sector.

1.1. Previous Work

Energy disaggregation can be applied at loads in the residential sector (Zhao et al., 2019), as well as in the commercial sector (Ling et al., 2021). In both cases, a sensor is required. When a sensor is needed for each individual (load) appliance, it is known as intrusive load monitoring (ILM) (Ridi et al., 2014). The term non-intrusive load monitoring (NILM) (Norford and Leeb, 1996) is used when only one sensing point is required in order to sense the end-use of energy, thus involving no need for intrusion onto the energy customer's property. In both methods of monitoring, features are required to distinguish between the considered loads. In ILM, the hardware is complicated but the software is simple. In NILM, the hardware is simple but a complex signal processing is utilized to extract the features (Kang et al., 2022). Different features have been proposed in the previous work extracted from one of three analysis modes: steady-state mode (Hart, 1992), transient mode (Liang et al., 2009), and hybridization between steady-state and transient modes (Chang et al., 2012). Different machine learning algorithms (MLA) have been utilized in the relevant work to develop an appropriate prediction model (Rehman et al., 2021). MLAs have been trained in the previous work based on both supervised learning (Moreno Jaramillo et al., 2020) and unsupervised learning (Thokala et al., 2022). Nevertheless, load disaggregation using a single point sensing on fast charging stations has not been considered in the related studies.

1.2. Aim of the Study

The objective of this paper is to fill the research gap by applying load disaggregation using a single point sensing on fast charging stations (FCSs) to increase the capability and the effectiveness of any energy management program applied at the FCSs.

2. Methodology

2.1. Modelling and Modification of the Distribution Test System

The IEEE 4 bus test system is considered in this work (Schneider et al., 2017). The nominal voltage of the system is 12.47 kV. The source voltage steps down to the distribution voltage level of 4.16 kV in order to feed the connected load via a one 3-phase transformer bank. The secondary of the distribution transformer is configured as a delta connection to feed the connected load at a distance of 2,500 ft. The distribution transformer is rated 6000 kVA whereas the spot load of each line-to-line is rated as 1.5 MVA, 2 MVA, and 2.5 MVA, at 0.85, 0.9, and 0.9 lagging power factor, respectively. The configurations of the secondary of the distribution transformer as well as the spot load are modified to be balanced Wye connected. Furthermore, a commercial facility (a supermarket) and FCSs are integrated to the distribution test system, as shown in Fig 1. Therefore, the total load fed by the transformer is 5400 kW at 0.9 lagging power factor.

2.2. Connection of Fast Charging Stations

At the point of common coupling (PCC), four FCSs are connected to the test system via four distribution transformers. Each transformer (T_i) is connected to an FCS_i via a Br_i breaker, where i indicates the FCS number. Each FCS_i operates at nominal voltage 0.480 kV. Thus, each T_i transformer steps down the primary voltage of 4.16 kV to 0.480 kV.

Each Br_i breaker has two states of operation: on and off. The state "on" indicates that the breaker S_i is closed and thus the FCS_i is occupied. The state "off" means that the breaker Br_i is open and thus the FCS_i is idle.

2.3. Connection of a Commercial Load

2.3.1. Reason for Inclusion

The number of charging events occurred at an FCS may be affected by the location of that FCS (Alshareef, 2022). The proposed commercial load in this study is a supermarket that is connected to the test system at the PCC from which FCSs are integrated. The assumption is that the four FCSs are located at the supermarket parking lot. The aim is to disaggregate the total load at the PCC. The supermarket includes different centers providing different services whereby their hours of operation are varied, which results in varying their power consumption at the PCC. Therefore, the supermarket is considered as a background load whereas its varying power consumption at the PCC may disturb extracting the patterns from the feature space and, consequently, detecting the events of FCSs.

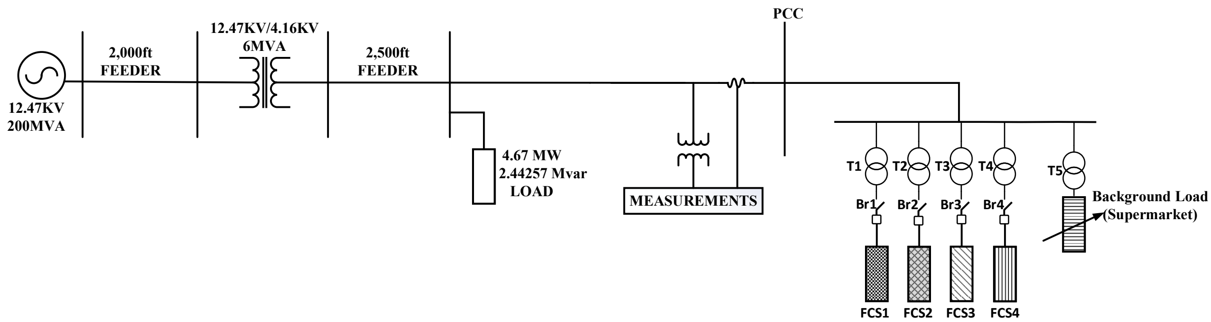

Fig. 1. Modified IEEE 4 bus standard test feeder.

2.3.2. Commercial Load Profile

The supermarket benchmark models are developed by the U.S. Department of Energy (DOE) represented by annual load profiles in kW estimated at an hourly basis (8760 hours) (Deru et al., 2011). The models describe the supermarket profiles in 936 cities located in 50 states characterized by one or more climate zones, based on the geographic coordinates (Alshareef and Morsi, 2017). Three steps are required in order to utilize the load profile of the supermarket, namely: data collection, data processing, and Monte Carlo simulation (MCS). For the first step, a load matrix of 8760 rows and 936 columns is generated to include all the profiles from all the cities where the number of rows corresponds

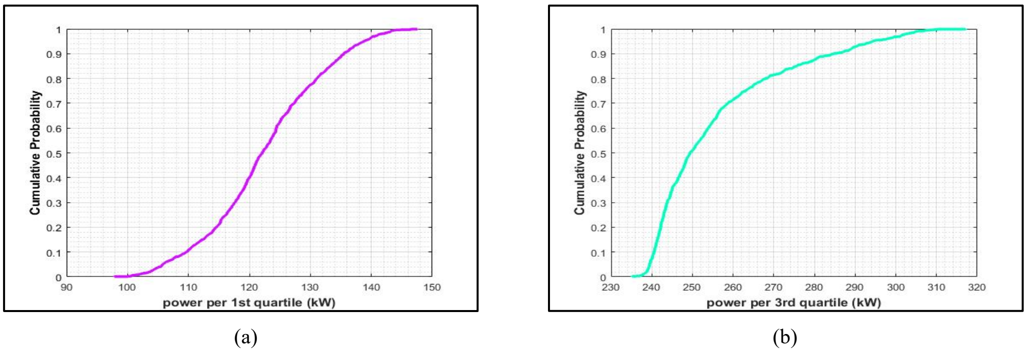

(a) (b)

Fig. 2. Cumulative distribution functions. (a) kW power of the 25th; (b) kW power of the 75th.

to the number of hours in a year while the number of columns indicates the cities. Subsequently, from each column in the data matrix, the 25th and 75th percentiles are calculated to generate the empirical cumulative distribution functions of each quartile. An MCS is then used in this step to generate two uniform random variables. The inverse transform method is adopted to estimate the lower and upper bounds of the kW power of the supermarket from the generated random variables as well as the empirical cumulative functions of the 1st and 3rd quartiles, respectively. Given the values of the lower and upper bounds, a uniform random number is generated to represent the demand of the supermarket seen at the PCC at that instance of time. The kW power of the 25th and 75th percentiles is depicted in Fig. 2 as well as their empirical cumulative distribution functions.

2.4. Fourier Transform

The Fourier transform (FT) is formulated mathematically as follows (Weeks, 2007):

$$\mathrm{X}(\kappa) = \int_{-\infty}^{\infty} \chi(t).\, e^{-j\omega_\kappa t} dt \tag{1}$$

When the FT is applied to discrete waves, it is called the Discrete Fourier Transform (DFT) and formulated mathematically as (Weeks, 2007):

$$\mathrm{X}[\kappa] = \sum_{n=0}^{N-1} \chi[n].\, e^{-j\omega_\kappa n} \tag{2}$$

where $\mathrm{X}[\kappa]$ is the discrete Fourier transform of the discrete time signal $\chi[n]$, evaluated over a range of values of κ from 0 up to $N/2$, κ is an integer called the bin number, e is the Euler's number, $\omega_\kappa = 2\pi\kappa/N$ is the frequency associated with bin κ, radians per sample, N is the number of samples of the discrete time signal $\chi[n]$ being analysed. The active, reactive, and apparent power at the fundamental frequency of each phase R, S, and T can be determined by applying the DFT to the three-phase voltage and current waveforms as follows (Ribeiro et al., 2013):

$$P_{j1} = V_{j1} I_{j1} \cos \gamma_j \tag{3}$$

$$Q_{j1} = V_{j1} I_{j1} \sin \gamma_j \tag{4}$$

$$S_{j1} = V_{j1} I_{j1} \tag{5}$$

where j is an index for each phase (i.e., R, S, and T), (V_{j1} and I_{j1}) are the root mean square value of the voltage and the current at the power system frequency, respectively. γ_j is the phase angle displacement and ($P_{j1}, Q_{j1}$and S_{j1}) is the active, reactive, and apparent power, respectively.

2.5. Feature Selection

After decomposing the original time domain signals, features are extracted and utilized to disaggregate the different charging events at the FCSs. Instead of using the fundamental power components, the change in the power components is utilized. Thus, changes of the active ($\ddot{P}$), reactive ($\ddot{Q}$), and apparent ($\ddot{S}$) power are determined as in equations (8)-(10) and utilized to build the attribute matrix. The attribute matrix is used as input to the classification system.

$$\ddot{V}_j[n] = v_j[n] - v_j[n - \mathcal{S} - 1] \tag{6}$$

$$\ddot{I}_j[n] = \iota_j[n] - \iota_j[n - \mathcal{S} - 1] \tag{7}$$

$$\ddot{P}_j[n] = P_j[n] - P_j[n - 1] \tag{8}$$

$$\ddot{Q}_j[n] = Q_j[n] - Q_j[n - 1] \tag{9}$$

$$\ddot{S}_j[n] = S_j[n] - S_j[n - 1] \tag{10}$$

where $\jmath$ is an index for each phase (i.e., R, S, and T), $P_{\jmath}[n]$, $Q_{\jmath}[n]$ and $S_{\jmath}[n]$ indicate , respectively, the values of the power components of the $\jmath^{th}$ phase, at the n^{th} instant, $P_{\jmath}[n-1], Q_{\jmath}[n-1]$ and $S_{\jmath}[n-1]$ are values of the fundamental power components calculated using the voltage, $v_{\jmath}[n-\mathcal{S}-1]$, and current, $\iota_{\jmath}[n-\mathcal{S}-1]$, values sampled one cycle ago, where $\mathcal{S}$ is the number of samples per cycle.

2.6. Machine Learning Techniques

Load disaggregation requires differentiating between individual appliances and their combinations. As a result, these loads need to be classified at the individual device level. After extracting the fast chargers' features, a machine learner should be introduced and trained using these features for generalization. When classes of these features are unknown, the machine learner is known as unsupervised learning. When classes of these features are known, the machine learner is termed as supervised learning. In this paper, known data and their responses are fed to a classifier in order to be trained based on these inputs. This classifier is then utilized to predict the classes for unseen data.

2.6.1. Kernel Naïve Bayes Classifier

The first proposed classifier is the Kernel Naive Bayes (KNB). The kernel function can be chosen to reflect the nature of the data and the problem being solved. Some common kernel functions include radial basis functions, polynomial functions, and sigmoid functions. Once the data has been mapped onto the high-dimensional feature space, the Naive Bayes algorithm is applied to classify the data. The algorithm works by estimating the probability distribution of each class and then using the Bayes' theorem to calculate the probability that a new event belongs to each class. The class with the highest probability is then assigned to the new event (Murakami and Mizuguchi, 2010).

2.6.2. k-Nearest Neighbors Classifier

Let m represent the number of attributes; each record is then represented by the k-Nearest Neighbors (KNN) classifier as a data point in the m-dimensional space. In order to classify a new record, the proximity of that new record to each data point in the training data set is computed using a proximity measure (i.e., the Euclidean distance). The Euclidean distance ($\mathcal{U}$) between two points p and q is given as (Laaksonen and Oja, 1996):

$$\mathcal{U}(p,q) = \sqrt{\sum_{k=1}^{m}(p_k - q_k)^2} \tag{11}$$

where m is the number of dimensions, p_k is the k^{th} components of p, and q_k is the k^{th} attributes of q.

2.7. Performance Metrics

The accuracy of a machine learning classification model is computed as the ratio of the number of instances that classified accurately with the total number of instances, as in (12). The confusion matrix is a tool commonly used in machine learning to evaluate the performance of a classifier. Table 1 shows the confusion matrix of two variables. Accuracy for models is computed based on the confusion matrix as the ratio of numbers of instances that classify accurately with the total number of instances. Precision and recall are two additional metrics that are calculated from the confusion matrix to evaluate the performance of the classifier. Given that, precision and recall are calculated, respectively, as in (13) and (14) (Tan et al., 2016).

Table 1. Confusion matrix for a 2-class problem.

		Actual Class	
		Positive	Negative
Predicted class	Positive	True Positive (TP)	False Positive (FP)
	Negative	False Negative (FN)	True Negative (TN)

$$Accuracy, \mathcal{A}cc = \frac{TP+TN}{TP+FP+FN+TN} \times 100 \tag{12}$$

$$Precision, \mathfrak{p} = \frac{TP}{TP+FP} \tag{13}$$

$$Recall, \mathfrak{r} = \frac{TP}{TP+FN} \tag{14}$$

The evaluation depends on the F-measure ($\mathfrak{T}$), which combines both precision ($\mathfrak{p}$) and recall ($\mathfrak{r}$) to measure the extent to which a cluster includes only instances of a particular class and all instances of that class (Powers, 2020). The F-measure is calculated as:

$$\mathrm{F-measure}, \mathfrak{T} = \frac{2\times\mathfrak{p}\times\mathfrak{r}}{\mathfrak{p}+\mathfrak{r}} \tag{15}$$

3. Simulation Results and Discussion

3.1. Case Study

In order to recharge an EV via a fast charger, any breaker Br_i, shown in Fig. 1, has to be turned "ON" in order to connect the charger to the distribution grid. When any breaker Br_i is turned "ON", it means that the slot is occupied by an EV and a charging event is considered, based on the turned "ON" state. A large number of scenarios are simulated in this case. The generated scenarios are dependent on the breakers' states. In each scenario, one breaker will be switched on at time t while the rest of the breakers will have been switched on and/or off in advance. Furthermore, the profile of the commercial load (the supermarket) is estimated as explained in section 2.3.2 The total number of applied scenarios is 864 cases, resulting from the sum of: four fast chargers × eight possible combinations × five cases of harmonic distortion (adding the 5th harmonic in 1% step, from 1% to 5%) × 11 cases of frequency variation (in 1Hz step, from 55Hz to 65Hz) × 11 cases of voltage magnitude variation (in 1% step, from -5% to 5%). Half of the applied scenarios are utilized for training the classifiers while the other half are for the evaluation.

3.2. Training and Testing Data Sets

Each classifier was trained using the same data set consisting of 432 cases generated under different power quality disturbances, such as harmonic distortion, frequency variations, and volage magnitude variations. Also, in each generated case, MCS is applied to estimate the commercial load profile, which represents another disturbance for charging event disaggregation. After developing the machine learning models using the charging events, each classifier is tested using the testing data set to predict their classes. The testing data set consists of 432 cases generated under similar scenarios as applied to the training data set.

3.3. Performance Evaluation of the Turn-on Event of Fast Charging Stations

The performance of the proposed model is evaluated using the classification accuracy metric. Moreover, precision, recall, and the F-score are utilized for assessing the performance in order to overcome the imbalanced classification problem in the data set. In the classification process, one FCS is considered as a true positive class and the absolute classification accuracy for that class is determined accordingly, as depicted in Table 2. The results reveal that, in the case of FCS_4, both classifiers provide 100% classification accuracy while the lowest classification accuracy is achieved in the case of FCS_2 (rated 90 kW), where the KNB and KNN provide 93.52% and 62.03%, respectively. Further, the mean classification accuracies obtained by the KNB and KNN are determined as 99.3% and 87.2%, respectively. The results for precision and recall for both classifiers are presented in Fig. 3. Achieving high absolute classification accuracy for each individual positive class positively impacts the results of precision and recall, as shown in Fig. 3. As the per unit values of the precision and recall increase, the classifier is able to predict most of the true positive and true negative classes. Given the values of precision and recall, the value of the F-score is computed as shown in Fig.

4. The results of the F-measure illustrate that the KNN achieved the lowest classification accuracy to classify the FCS_2. The FCS_4 is able to correctly predict all cases, thus the value of the F-measure is 1. In the case of the KNB as depicted in Fig. 4, values of the F-measure for all classes are above 0.94, indicating that the KNB outperforms the KNN based on the mean classification accuracy as well as the F-measure index.

Table 2. Confusion matrix using both classifiers.

	Positive Classes				
	FCS_1	FCS_2	FCS_3	FCS_4	Mean
Kernel Naïve Bayes	95.37	93.52	100	100	99.3%
k-Nearest Neighbors	95.37	62.03	91.67	100	87.2%

It is worth mentioning that the commercial load (the supermarket), as presented in Fig. 1, is acting as a background load whose profile is estimated randomly based on empirical cumulative distribution functions using MCS. Thus, the power consumption of the supermarket may overlap with the output power of FCS_2 and cause degrading of the performance of the classifier, as in the case of the KNN.

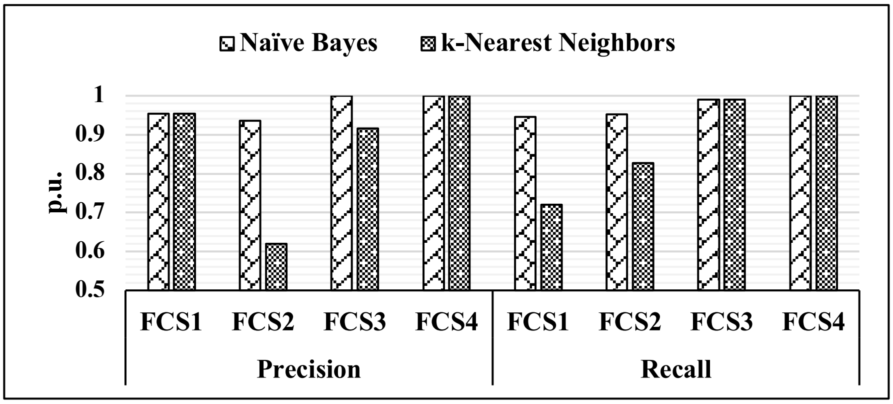

Fig. 3. Precision and Recall values for KNBC and KNNC.

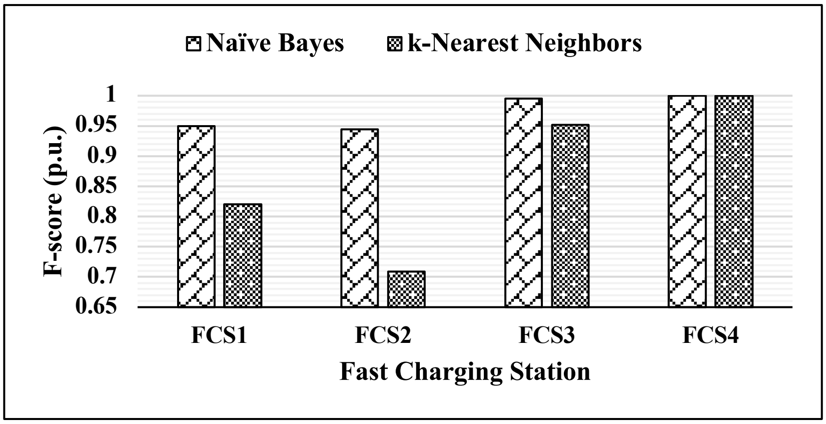

Fig. 4. F-measure for disaggregation of different fast chargers using KNBC and KNNC.

4. Conclusion

This paper applies load disaggregation at fast charging stations that consist of four slots that vary in their rated power from 50 kW to 350 kW. The charging station is located at the parking lot of a commercial facility (a supermarket) whereas both loads are fed by the main grid at the point of common coupling. The Monte Carlo simulation method is utilized to estimate probabilistically the load profile of the supermarket. The results have shown that the power signature can be utilized in disaggregating the output power of the four EV fast chargers considered in this study, using the appropriate machine learning classifier. However, the power variation caused by the commercial load (the supermarket) at the point of common coupling may disturb the disaggregation process by overlapping with the output power of the fast chargers causing the performance of the classifiers to degrade.

Acknowledgements

Sami M. Alshareef extends his appreciation to Prince Nawaf bin Abdulaziz Chair for funding the current work.

References

Alshareef, S.M., 2022. A Novel Fairness-Based Cost Model for Adopting Smart Charging at Fast Charging Stations. Sustainability 14. https://doi.org/10.3390/su14116450

Alshareef, S.M., Morsi, W.G., 2017. Probabilistic commercial load profiles at different climate zones 1–7. https://doi.org/10.1109/epec.2017.8286233

Chang, H.-H., Chen, K.-L., Tsai, Y.-P., Lee, W.-J., 2012. A New Measurement Method for Power Signatures of Nonintrusive Demand Monitoring and Load Identification. IEEE Trans. on Ind. Applicat. 48, 764–771. https://doi.org/10.1109/TIA.2011.2180497

Deru, M., Field, K., Studer, D., Benne, K., Griffith, B., Torcellini, P., Liu, B., Halverson, M., Winiarski, D., Rosenberg, M., 2011. US Department of Energy commercial reference building models of the national building stock.

Hart, G.W., 1992. Nonintrusive appliance load monitoring. Proceedings of the IEEE 80, 1870–1891.

Kang, J.-S., Yu, M., Lu, L., Wang, B., Bao, Z., 2022. Adaptive Non-Intrusive Load Monitoring Based on Feature Fusion. IEEE Sensors Journal 22, 6985–6994.

Laaksonen, J., Oja, E., 1996. Classification with learning k-nearest neighbors. Presented at the Proceedings of international conference on neural networks (ICNN'96), IEEE, pp. 1480–1483.

Liang, J., Ng, S.K., Kendall, G., Cheng, J.W., 2009. Load signature study—Part I: Basic concept, structure, and methodology. IEEE transactions on power Delivery 25, 551–560.

Ling, Z., Tao, Q., Zheng, J., Xiong, P., Liu, M., Xiao, Z., Gang, W., 2021. A Nonintrusive Load Monitoring Method for Office Buildings Based on Random Forest. Buildings 11, 449. https://doi.org/10.3390/buildings11100449

Moreno Jaramillo, A.F., Laverty, D.M., Del Rincon, J.M., Hastings, J., Morrow, D.J., 2020. Supervised Non-Intrusive Load Monitoring Algorithm for Electric Vehicle Identification, in: 2020 IEEE International Instrumentation and Measurement Technology Conference (I2MTC). Presented at the 2020 IEEE International Instrumentation and Measurement Technology Conference (I2MTC), IEEE, Dubrovnik, Croatia, pp. 1–6. https://doi.org/10.1109/I2MTC43012.2020.9128529

Murakami, Y., Mizuguchi, K., 2010. Applying the Naïve Bayes classifier with kernel density estimation to the prediction of protein–protein interaction sites. Bioinformatics 26, 1841–1848.

Norford, L.K., Leeb, S.B., 1996. Non-intrusive electrical load monitoring in commercial buildings based on steady-state and transient load-detection algorithms. Energy and Buildings 24, 51–64. https://doi.org/10.1016/0378-7788(95)00958-2

Powers, D.M., 2020. Evaluation: from precision, recall and F-measure to ROC, informedness, markedness and correlation. arXiv preprint arXiv:2010.16061.

Rehman, A.U., Lie, T.T., Vallès, B., Tito, S.R., 2021. Comparative evaluation of machine learning models and input feature space for non-intrusive load monitoring. Journal of Modern Power Systems and Clean Energy 9, 1161–1171.

Ribeiro, P.F., Duque, C.A., Ribeiro, P.M., Cerqueira, A.S., 2013. Power systems signal processing for smart grids. John Wiley & Sons.

Ridi, A., Gisler, C., Hennebert, J., 2014. A survey on intrusive load monitoring for appliance recognition, in: 2014 22nd International Conference on Pattern Recognition. IEEE, pp. 3702–3707.

Schneider, K.P., Mather, B., Pal, B., Ten, C.-W., Shirek, G.J., Zhu, H., Fuller, J.C., Pereira, J.L.R., Ochoa, L.F., de Araujo, L.R., 2017. Analytic considerations and design basis for the IEEE distribution test feeders. IEEE Transactions on power systems 33, 3181–3188.

Tan, P.-N., Steinbach, M., Kumar, V., 2016. Introduction to data mining. Pearson Education India.

Thokala, N.K., Paresh, S., Chandra, M.G., 2022. An effective electrical load disaggregation approach for low-sampled smart meter data, in: Proceedings of the 9th ACM International Conference on Systems for Energy-Efficient Buildings, Cities, and Transportation, BuildSys '22. Association for Computing Machinery, New York, NY, USA, pp. 149–158. https://doi.org/10.1145/3563357.3564070

Weeks, M., 2007. Digital signal processing using MATLAB and wavelets. Infinity Science Press, Hingham, Mass.

Zhao, H., Yan, X., Ma, L., 2019. Training-free non-intrusive load extracting of residential electric vehicle charging loads. IEEE Access 7, 117044–117053.